

Pathogenesis and Staging of Craniovertebral Tuberculosis: Radiographic Evaluation, Classification, and Natural History

Global Spine Journal
2023, Vol. 13(8) 2155–2167
© The Author(s) 2022
Article reuse guidelines:
sagepub.com/journals-permissions
DOI: 10.1177/21925682221074671
journals.sagepub.com/home/gsj



Kshitij Chaudhary, MBBS MS FACS¹ , Zach Pennington, MD^{2,3} ,
Ashok K. Rathod, MBBS MS⁴, Vinod Laheri, MBBS MS⁵, Mihir Bapat, MBBS MS⁵,
Daniel M. Sciubba, MD MBA^{2,6} , and Sanjeev J Suratwala, MD^{6,7} 

Abstract

Study Design: Retrospective cohort.

Objective: To radiographically evaluate Craniovertebral junction (CVJ) tuberculosis infection pathogenesis and to propose a modification to the Lifeso classification.

Methods: A cohort of patients with radiologically or microbiologically identified CVJ tuberculosis treated at a single tertiary referral center in a TB endemic area was queried for characteristics about clinical presentation, treatment, and radiographic evidence of bone destruction and abscess formation were included. Disease was classified according to the Lifeso grading system and bony lesions were classified as either type I (preservation of underlying structure) or type 2 (damage of underlying structure).

Results: 52 patients were identified (mean age 28.5 ± 13.4yr, 48% male; 14% with a prior history of tuberculosis). All presented with neck pain at presentation, 29% with rotatory pain, and 37% with myelopathy. Comparison by Lifeso type showed Lifeso III lesions had longer symptom durations ($P = .03$) and more commonly had periarticular or prepedal abscess formation ($P < .05$), spinal cord compression ($P < .01$), and more commonly involved the C2 body and atlanto-dental joint. Underlying bony destruction was more common for lesions of the lateral atlantoaxial joints and atlanto-dental joints in Lifeso III cases than in either Lifeso I or II (all $P < .05$).

Conclusions: The radiologic findings of the present series suggest CVJ TB infection may originate in the periarticular fascia with subsequent invasion into the adjacent atlanto-dental and lateral atlantoaxial joints in later disease. To reflect this proposed etiology, we present a modified Lifeso classification to describe the radiologic pathogenesis of CVJ TB.

Keywords

craniovertebral junction, atlantoaxial instability, tuberculosis, osteomyelitis

Background

First reported by Kracht in 1950,¹ tuberculosis (TB) infection of the craniovertebral junction (CVJ) is rare and accounts for less than 1% of all spinal tuberculosis.²⁻⁴ The spectrum of radiological presentation of CVJ TB ranges from abscess formation to frank atlantoaxial instability with proximal translocation of the odontoid.⁵ Similarly, clinical presentation varies from neck pain with stiffness to severe neurological deficits due to upper cervical spinal cord compression.^{3,6,7}

The management of CVJ TB is controversial. It is clear that uncomplicated early infections can be treated effectively with anti-tuberculosis chemotherapy and that severe neurological deficits in later stages of the disease require surgery. However, there is

¹Department of Orthopaedic Surgery, PD Hinduja Hospital and Medical Research Centre, Mumbai, India

²Department of Neurosurgery, Johns Hopkins University School of Medicine, Baltimore, MD, USA

³Department of Neurosurgery, Mayo Clinic, Rochester, Rochester, MN, USA

⁴Department of Orthopaedics, Lokmanya Tilak Municipal Medical College and General Hospital, Mumbai, India

⁵Department of Orthopaedics, King Edward VII Memorial Hospital, Mumbai, India

⁶Department of Neurosurgery, Zucker School of Medicine at Hofstra, Long Island Jewish Medical Center and North Shore University Hospital, Northwell Health, Manhasset, NY, USA

⁷Department of Orthopaedic Surgery, New York Orthopaedic and Spine Center, Northwell Health, Great Neck, NY USA

Corresponding Author:

Kshitij Chaudhary, Department of Orthopaedic Surgery, PD Hinduja Hospital and Medical Research Centre, SVS Rd, Mahim West, Shivaji Park, Mumbai, Maharashtra 400016, India.
Email: chaudhary.kc@gmail.com



Creative Commons Non Commercial No Derivs CC BY-NC-ND: This article is distributed under the terms of the Creative Commons Attribution-NonCommercial-NoDerivs 4.0 License (<https://creativecommons.org/licenses/by-nc-nd/4.0/>) which permits non-commercial use, reproduction and distribution of the work as published without adaptation or alteration, without further permission provided the original work is attributed as specified on the SAGE and Open Access pages (<https://us.sagepub.com/en-us/nam/open-access-at-sage>).

controversy over how best to treat patients who present with significant instability or deformity but do not have a neurological deficit. Some suggest conservative therapy irrespective of the destruction and deformity,^{6,8} while others suggest aggressive surgical debridement and stabilization.⁹ Several treatment algorithms have been published. However, the usefulness of these classifications is limited by their complexity or failure to account for the deformities, such as proximal translocation of the odontoid, often seen in this infection.^{3,6,7}

As with any disease, a fair understanding of the pathogenesis of CVJ TB infection is mandatory to propose a rational treatment algorithm that is inclusive of all possible clinical-radiological presentations. To our knowledge, there are no studies that explain the pathogenesis of CVJ TB. Therefore, in this study, we hope to piece together a chain of events that illustrate the pathogenesis of CVJ TB by analyzing MRIs of patients who presented to us in different stages of the infection. Armed with this knowledge, we propose modifications to the Lifeso staging system,¹⁰ which is the most popular radiological staging classification in the literature.

Methods

After obtaining institutional approval, we retrospectively reviewed a series of 68 consecutive patients treated for CVJ tuberculosis at a single center over a 12-year period. The IRB deemed the present study as not meeting the definition of humans subjects research. The diagnosis of CVJ TB was based either on microbiological confirmation by a positive culture of *Mycobacterium tuberculosis* (n = 18), or histopathological evidence of caseating granulomas (n = 28). For those with inconclusive biopsy (n = 22), the diagnosis was based on typical clinico-radiological presentation with a positive response to anti-tuberculous therapy, as used by other groups.^{3,11} Tissue/abscess sampling was performed via a transoral or CT-guided biopsy for conservatively treated patients, or via intraoperative open biopsy in those treated surgically. Ten patients were excluded from the analysis due to inadequate documentation of pre-treatment records. In addition, 6 patients did not have any recorded follow-up visits, and were not included in the analysis. The remaining 52 patients with a minimum of 2 years of follow-up were included and are reported in the analysis.

Clinical Records

Data was collected regarding presenting symptoms and signs. Neurological involvement was graded using Frankel grades.¹² All patients, with the exception of 4 patients with multidrug-resistant infection, were treated with a standard regimen of anti-tuberculosis therapy (ATT) for 9–12 months as recommended by the consulting infectious disease specialist.

Imaging Records

Pre-treatment imaging includes AP and lateral cervical spine radiographs and magnetic resonance imaging (MRI) in all

patients. T1-weighted and T2-weighted sagittal and axial images, and short-tau inversion recovery (STIR) coronal images were available in all patients. CT scans were also obtained by the treating physician when it was felt clinically necessary (n = 38). Dynamic C-spine radiographs to assess atlantoaxial instability (AAI) were attempted in all patients. Only extension views were attempted in those with neurological deficits [to assess reducibility], while flexion and extension views were attempted in all other patients. For all patients with evidence of subluxation on lateral films, we also attempted reduction with traction under anesthesia. This was used as the ultimate classifier for instability in the present series.

Volumetric images were interpreted by 2 surgeons and a fellowship-trained neuroradiologist with discrepancies resolved by consensus. Fifteen anatomical regions were examined for evidence of osteomyelitis, with each graded as type 1 (preserved regional structure and function) or type 2 (lesions with associated structural collapse). Bony lesions were additionally classified as having articular surfaces (i.e., occipital condyles, C1 lateral masses, C1 anterior arch, odontoid, C2 superior facets) or lacking articular surfaces (i.e., clivus, occipital squama, posterior C1 arch, C2 arch, C2-4 bodies). Abscess location was documented with respect to the pre-vertebral fascia, buccopharyngeal fascia, and dura.

Instability

Instability was classified as antero-posterior (AP), rotational, or vertical. AP instability was defined by an increase in atlanto-dental interval (ADI) of > 3 mm (adults) or > 5 mm (children < 12 years old). In patients with either odontoid or C1 arch destruction, AP instability was defined by anterior translation of the posterior arch with respect to the spinolaminar line.¹³ Rotatory instability was subclassified as with or without concomitant AP instability. Vertical instability or proximal translocation of the odontoid (basilar impression) was diagnosed when the tip of odontoid process was above the McRae line.¹⁴ In cases with odontoid destruction, vertical instability was diagnosed by noting the position of the projected tip of the odontoid process in relation to the McRae line (Figure 2).

Statistical Analysis

Data was collected using Microsoft Excel (Redmond, WA) and analyzed using Statistic v13.3 (TIBCO, Palo Alto, CA). Data is reported as mean ± standard deviation for continuous variables and counts with percentages for ordinal, dichotomous, and categorical variables. Univariable statistics were performed using Mann–Whitney U tests for continuous data, Fisher-exact tests for dichotomous variables, and χ^2 tests for categorical data. Clinical symptoms and bony involvement were compared between Lifeso stage I, II, and III lesions using analysis of variance (ANOVA) χ^2 tests. Pairwise comparisons

were made using Fisher-exact tests and Tukey tests for honest significant differences. Statistical significance was defined by $P < .05$.

Results

Clinical Presentation

Of the 52 patients (Table 1), mean age was 28.5 ± 13.4 years, 48.1% were male, and 13.5% had a known history of tuberculosis prior to presentation. Average symptom duration at presentation was 4.0 ± 2.3 months. All patients presented with pain and stiffness in the neck, and 15 (28.8%) had torticollis. Nineteen (37%) of patients had symptoms of myelopathy at baseline, with an average duration of 0.8 ± 0.8 months. Two patients had hypoglossal nerve palsy and 3 patients presented with shortness of breath and dysphagia due to large prevertebral abscesses.

Abscess Localization

Forty-seven patients (90.3%) had radiographic evidence of abscesses with 5 (9.6%) having only granulation tissue surrounding the CVJ. In all patients, the abscesses or granulation tissue were located within the confines of the prevertebral fascia investing the cervical vertebrae and paraspinous muscles (Figure 1A-G). Extension of the prevertebral abscess to the epidural space (25%), posterior aspect of the CVJ (19.2%), and posterior triangle of the neck were noted (23.1%). However, abscesses were never located in the retropharyngeal space, bounded by the buccopharyngeal and prevertebral fascial layers, and remained within the confines of the deep layer of the deep cervical fascia prevertebral fascia).

Localization of Osteomyelitis

Of the 780 possible anatomical sites (15 sites/patient \times 52 patients), 321 (41%) had radiological evidence of osteomyelitis. Of these 321 sites, 254 (79.1%) were classified as type 1 and 67 (20.8%) as type 2. The most common site of involvement was the odontoid (92.3%) followed by the C1 lateral masses, C2 body, and C2 superior faces, anterior C1 arch, and occipital condyles. Anatomical areas that did not contribute to the synovial joints of the occipitocervical and atlantoaxial regions were infected at much lower rates than those with articulating surfaces (15.9 vs 62.9%; Table 1). Type 2 lesions were significantly more common in regions with articulating surfaces than in those without articulating surfaces (14.4% vs 1.9%; $P < .01$), suggesting that articular surfaces were more severely involved.

Instability

Eighteen (34.6%) of patients did not have any demonstrable instability, whereas 34 (65.4%) had antero-posterior (AP)

Table 1. Demographics, treatment, and outcomes of the 52 included patients.

Variable	Mean \pm SD	n (%)
Demographics		
Age (yr)	28.5 ± 13.4	—
Sex (% male)	—	25 (48.1)
History of TB prior to presentation	—	7 (13.5)
Symptoms		
Duration of symptoms (mo)	4.0 ± 2.3	—
Pain	—	52 (100)
Pain with rotation	—	15 (28.8)
Torticollis	—	15 (28.8)
CN XII dysfunction	—	2 (3.8)
Dysphagia	—	4 (7.7)
Respiratory distress	—	3 (5.8)
Myelopathy	—	19 (36.5)
Preoperative Frankel Score		
E	—	33 (63.5)
D	—	7 (13.5)
C	—	8 (15.3)
B	—	4 (7.7)
A	—	0 (0)
Bladder sphincter dysfunction	—	8 (15.4)
Bowel sphincter dysfunction	—	3 (5.8)
Duration of neuro deficits (mo, n = 19)	—	0.8 ± 0.8
Radiographic data		
<i>Lifeso Stage</i>		
1	—	18 (34.6)
2	—	15 (28.8)
3	—	19 (36.5)
Abscess	—	47 (90.3)
Retropharyngeal	—	0 (0)
Prevertebral	—	47 (90.3)
Paravertebral	—	10 (19.2)
Preclival	—	39 (75)
Periodontoid/preidental	—	36 (69.2)
Posterior CVJ	—	10 (19.2)
Epidural space	—	13 (25)
Posterior triangle of neck	—	12 (23.1)
Spinal cord signal change	—	12 (23.1)
<i>Bone involvement</i>		
780 sites		
# Of articular surfaces involved (n = 416)	—	262 (62.9)
# Of nonarticular surfaces involved (n = 364)	—	58 (15.9)
<i>Instability</i>		
ADI (mm)	5.7 ± 4.0	—
Anterior dislocation	—	34 (65.4)
Rotatory dislocation	—	15 (28.8)
Vertical dislocation	—	10 (19.2)

Key: CVJ—craniovertebral junction; hr—hour; IOBL—intraoperative blood loss; mL—milliliter; mm—millimeter; mo—month; SD—standard deviation; yr—year; §Patient who died during perioperative period had preoperative neurological deficit and preoperative torticollis.

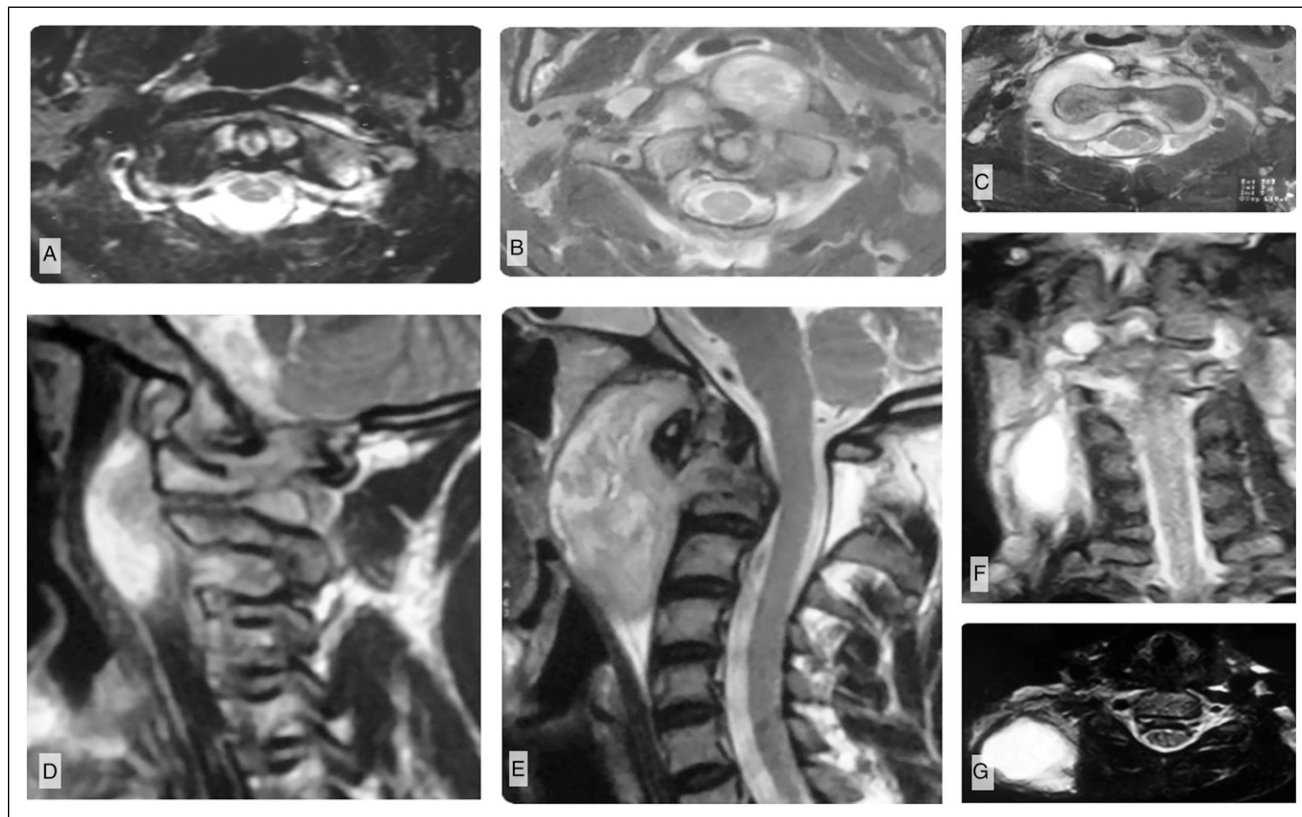


Figure 1. Abscess localization. (A) Axial T2-weighted MRI of patient with early-stage disease shows abscess formation within the prevertebral space, causing ventrally displacement of the prevertebral musculature (longus colli, longus capitis). (B) As the abscess expands, it predominately localizes around the synovial joints of the CVJ including the peridental region, (C) but it may also track laterally and through the neural foramina into the epidural space. (D, E) Sagittal T2-weighted MRI images demonstrate expansion of the prevertebral abscess, elevating the prevertebral muscles without violating the prevertebral fascia at any stage. (F) Coronal MRI showing a large, cold abscess that has tracked along the neurovascular bundles into the posterior triangle of the neck, which presents as a swelling on examination. (G) Axial MRI showing the same abscess in the posterior triangle of the neck.

translation suggesting instability. Of these 34 patients, 15 had AP instability due to incompetence of the transverse atlantal ligament (TAL), while the remaining 19 had instability due to bony destruction of the CRVJ joints. Of the latter 19, nine had AP instability due to pathological odontoid fracture ($n = 7$ or resorption of the odontoid process ($n = 2$)). The remaining 10 had additional vertical instability due to destruction of the lateral bony pillars of the CVJ, defined by the occipital condyles, C1 lateral masses, and C2 superior facets. Six of these had concomitant resorption of the odontoid process. Rotatory instability was observed in 15 patients (29%).

Based upon this, 3 distinct radiological stages were identified. Stage I lesions were those without radiographic instability within an intact TAL and intact CVJ bony structures. Stage II lesions showed AP instability without vertical instability. TAL incompetence was noted; however, the lateral bony pillars (occipital condyle-C1 lateral mass-C2 superior facet) and the atlanto-dental pivot joint structure were intact. In stage III, AP instability with or without vertical instability was noted. There was gross structural

damage to either the atlanto-dental pivot joints or lateral bony pillars. Rotatory deformity could occur in any stage; however, only in stages II and III is it accompanied by AP instability.

Analysis of Presentation by Lifeso Stage

Clinical Presentation. Comparisons of clinical characteristics showed several differences across the 3 stages (Table 2). Symptom duration was longest for stage III patients ($P = .03$). Rates of myelopathy were significantly higher amongst patients with stage II or III lesions as compared to stage I (both $P < .01$). None of the stage I patients presented with myelopathy, whereas 8 stage II patients (53%) and 11 stage III patients (57%) had evidence of myelopathy. In all cases, spinal cord compression was due to either instability, deformity, or a combination of the two. Of the 14 patients with epidural abscesses, 8 had myelopathy. However, in none of these patients could myelopathy be attributed to the epidural abscess alone, as all had concomitant instability or

Table 2. Comparison of clinical presentation, abscess location and bony involvement, and lesion severity by Lifeso stage in the 52 included patients.

	Lifeso Stage			Across Groups	Pairwise Comparison		
	I	II	III		I vs II	I vs III	II vs III
N	18	15	19	—	—	—	—
Demographics and clinical data							
Age (yr)	28.8 ± 11.0	26.5 ± 14.2	29.8 ± 15.1	.77	.87	.98	.76
Sex (M)	10 (55.6)	6 (40)	9 (47.4)	.67	.49	.75	.74
Symptom duration (mo)	3.5 ± 2.5	3.2 ± 1.4	5.1 ± 2.2	.03	.92	.08	.04
History of TB prior to presentation	3 (16.7)	1 (6.7)	3 (15.8)	.66	.61	>.99	.61
Clinical data							
<i>Clinical Symptoms</i>							
Pain	18 (100)	15 (100)	19 (100)	>.99	>.99	>.99	>.99
Pain with rotation	2 (11.1)	6 (40)	7 (36.8)	.12	.10	.12	>.99
Torticollis	3 (16.7)	5 (33.3)	7 (36.8)	.36	.42	.27	>.99
CN XII dysfunction	0 (0)	0 (0)	2 (10.5)	.16	>.99	.49	.49
Dysphagia	0 (0)	1 (6.7)	3 (15.8)	.19	.45	.23	.61
Respiratory distress	0 (0)	1 (6.7)	2 (10.5)	.38	.45	.49	>.99
Myelopathy	0 (0)	8 (53.3)	11 (57.9)	<.01	<.01	<.01	>.99
Frankel grade				<.01	<.01	<.01	.12
E	18 (100)	7 (46.7)	8 (42.1)				
D	0 (0)	3 (20)	4 (21.1)				
C	0 (0)	5 (33.3)	3 (15.8)				
B	0 (0)	0 (0)	4 (21.0)				
Bladder sphincter dysfunction	0 (0)	2 (13.3)	6 (31.6)	.03	.20	.02	.26
Bowel sphincter dysfunction	0 (0)	2 (13.3)	1 (5.3)	.26	.20	>.99	.57
Radiographic characteristics							
Abscess							
Periodontoid/pre dental	17 (94.4)	14 (93.3)	16 (84.2)	.52	>.99	.60	.61
Posterior CVJ	6 (35.3)	14 (100)	16 (100)	<.01	<.01	<.01	.61
Epidural space	1 (5.8)	2 (14.2)	7 (43.7)	.04	.58	.04	.24
Posterior triangle of neck	0 (0)	3 (21.4)	10 (62.5)	<.01	.08	<.01	.08
Granulation only	2 (11.7)	2 (14.2)	8 (50)	.05	>.99	.06	.13
Spinal cord signal change	1 (5.6)	1 (6.7)	3 (15.8)	.52	>.99	.60	.61
Epidural compression	0 (0)	4 (27.0)	8 (42.1)	<.01	.03	<.01	.48
	0 (0)	14 (93.3)	18 (94.7)	<.01	<.01	<.01	>.99
Bone involvement							
# Anatomical sites	270	225	285	—	—	—	—
# Nonarticular bony surfaces studied	126	105	133	—	—	—	—
# Nonarticular sites with OM	11 (8.7)	10 (9.5)	37 (27.8)	<.01	>.99	<.01	<.01
Clivus	1 (5.6)	3 (20)	6 (31.6)	.13	.31	.09	.70
Occipital squama	0 (0)	0 (0)	0 (0)	>.99	>.99	>.99	>.99
C1 posterior arch	0 (0)	0 (0)	1 (5.3)	.41	>.99	>.99	>.99
C2 body	8 (44.4)	6 (40)	19 (100)	<.01	>.99	<.01	<.01
C2 arch	1 (5.6)	1 (6.7)	2 (10.5)	.84	>.99	>.99	>.99
C3 body	1 (5.6)	0 (0)	6 (31.6)	.01	>.99	.09	.02
C4 body	0 (0)	0 (0)	2 (10.5)	.16	>.99	.49	.49
# Articular bony surfaces studied	144	120	152	—	—	—	—
# Articular sites with OM	77 (53.5)	76 (63.3)	109 (71.7)	<.01	.13	<.01	.15
R occipital condyle	8 (44.4)	6 (40)	9 (47.4)	.91	>.99	>.99	.74
L occipital condyle	6 (33.3)	9 (60)	9 (47.4)	.31	.17	.51	.51
C1 anterior arch	5 (27.8)	6 (40)	14 (73.6)	.02	.49	<.01	.08
R C1 LM	13 (72.2)	12 (80)	14 (73.7)	.86	.70	>.99	>.99
L C1 LM	13 (72.2)	13 (86.7)	16 (84.2)	.51	.41	.45	>.99

(continued)

Table 2. (continued)

	Lifeso Stage			Across Groups	Pairwise Comparison		
	I	II	III		I vs II	I vs III	II vs III
N	18	15	19	—	—	—	—
C2 dens	14 (77.8)	15 (100)	19 (100)	.02	.11	.05	>.99
R C2 superior facet	9 (50)	7 (46.7)	6 (31.6)	.48	>.99	.32	.48
L C2 superior facet	9 (50)	7 (46.7)	9 (47.4)	.98	>.99	>.99	>.99
Instability	2 (11.1)	15 (100)	19 (100)	<.01	<.01	<.01	>.99
ADI (mm)	2.0 ± 0.1	6.9 ± 2.5	8.3 ± 4.3	<.01	<.01	<.01	.39
Anterior dislocation	0 (0)	15 (100)	19 (100)	<.01	<.01	<.01	>.99
Rotatory dislocation	2 (11.1)	6 (40.0)	7 (36.8)	.12	.10	.12	>.99
Vertical dislocation	0 (0)	0 (0)	10 (52.6)	<.01	>.99	<.01	<.01
Bony involvement by stage							
<i>Articulating Bone</i>	0 (0)	2 (1.7)	58 (38.2)	<.01	.21	<.01	<.01
R occipital condyle	0 (0)	0 (0)	6 (31.6)	<.01	>.99	.02	.02
L occipital condyle	0 (0)	0 (0)	4 (21.1)	.02	>.99	.11	.11
C1 anterior arch	0 (0)	0 (0)	3 (15.8)	.06	>.99	.23	.24
R C1 LM	0 (0)	0 (0)	8 (42.1)	<.01	>.99	<.01	<.01
L C1 LM	0 (0)	1 (6.7)	9 (47.4)	<.01	.45	<.01	.02
C2 dens	0 (0)	0 (0)	15 (100)	<.01	>.99	<.01	<.01
R C2 superior facet	0 (0)	0 (0)	6 (31.6)	<.01	>.99	.02	.02
L C2 superior facet	0 (0)	1 (6.7)	8 (42.1)	<.01	.45	<.01	.05
<i>Nonarticulating Bone</i>	0 (0)	0 (0)	7 (5.3)	<.01	>.99	.01	.02
Clivus	0 (0)	0 (0)	1 (5.3)	.41	>.99	>.99	>.99
Occipital squama	0 (0)	0 (0)	0 (0)	>.99	>.99	>.99	>.99
C1 posterior arch	0 (0)	0 (0)	1 (5.3)	.41	>.99	>.99	>.99
C2 body	0 (0)	0 (0)	3 (15.8)	.06	>.99	.23	.24
C2 arch	0 (0)	0 (0)	0 (0)	>.99	>.99	>.99	>.99
C3 body	0 (0)	0 (0)	2 (10.5)	.16	>.99	.49	.49
C4 body	0 (0)	0 (0)	0 (0)	>.99	>.99	>.99	>.99

Key: CVJ—craniovertebral junction; L—left; LM—lateral mass; M—male; mm—millimeter; mo—month; OM—osteomyelitis; R—right; yr—year.

deformity. Three stage I patients had torticollis, due to either neck spasm or rotational instability without AP instability. In stage II and III, there were 5 (33.3%) and 7 (36.8%) with torticollis, which in all cases was due to a combination of rotational instability and either AP instability (stage II or III) or asymmetric bony pillar collapse (stage III only). Hypoglossal nerve palsy was seen only in Stage III, and both these patients had the palsy due to complete destruction of the occipital condyle through which this cranial nerve passes.

Abscess

While the rates of abscess formation (Table 2) did not differ between groups, abscesses appeared more expansile in higher stage lesions, with rates of periodontoid/pre dental abscesses being higher in stage II ($P < .01$) and III lesions ($P < .01$) than in stage I, and rates of periarticular and epidural abscess formation being more common in Stage III than in Stage I lesions ($P < .01$). Figure 1A-G shows abscess distribution and progression by comparison of

patients with early disease (Figure 1A) to late-stage disease (Figure 1F-G).

Osteomyelitis

Comparisons of bony involvement across the different stages are reported in Table 2. It was observed that the frequency of having one or more sites of articular bony involvement did not differ between groups ($P = .051$), whereas the proportion of patients with lesions in non-articular bone significantly differed between groups ($P < .01$). This suggests that regions with articulating surfaces are involved earlier in the disease process, and that infection spread to nonarticular bone as the disease progresses. Supporting this, it was noted that 65 of the 67 type 2 lesions were seen in stage III patients.

Rates of involvement of the C1 anterior arch ($P = .02$), odontoid process ($P = .02$), C2 body ($P < .01$), and C3 body ($P = .01$) all differed between groups. Comparison of stage I and II lesions showed no significant differences in rates of involvement; however, rates of C2 body ($P < .01$) and C3 body

Table 3. Modified Lifeso stages used for lesion classification.

	TAL	Structural Damage		Instability		
		<i>Atlanto-dental Pivot Joint</i>	<i>Lateral Bony Pillars</i>	<i>AP</i>	<i>Vertical</i>	<i>Rotatory</i>
Stage 1	Intact	—	—	—	—	+/-
Stage 2	Incompetent	—	—	+	—	+/-
Stage 3	Incompetent	+	+	+	+/-	+/-

Key:— = absent; + = present; AP = anterior-posterior; TAL—transverse atlantal ligament.

involvement ($P = .02$) were both higher in stage III than in stage II lesions. C1 anterior arch involvement ($P < .01$), odontoid involvement ($P = .05$), and C2 body involvement ($P < .01$) were all higher in stage III than in stage I lesions. Evaluating the severity of bony involvement (Table 2) suggested differences between groups in the severity involvement of the right ($P < .01$) and left occipital condyles ($P = .02$), right and left C1 lateral masses (both $P < .01$), odontoid process ($P < .01$), C2 body ($P < .01$), and right and left C2 superior facets (both $P < .01$). Pairwise comparisons showed that all significant differences were between stage III lesions and stage I or stage II lesions; none of the pairwise comparisons showed significant differences in severity of involvement between stage I and stage II lesions.

Discussion

Though tuberculosis affects nearly 10 million persons annually,¹⁵ less than 1% of cases will result in infection of the craniovertebral junction.^{16,17} CVJ TB can lead to neurological deterioration and craniocervical instability secondary to progressive destruction of the CVJ osseoligamentous elements. In the present study, we examined the natural progression of CVJ TB by evaluating radiographic and clinical differences between patients of different radiological stages.¹⁰ The results showed that markers of more advanced disease include the presence of abscess formation in the prevertebral and epidural space and progressively worse involvement of the median atlanto-dental pivot joint and lateral atlantoaxial and occipitoatlantal joints. Those with the most advanced disease tended to have the longest clinical prodromes and the most severe radiographic deterioration as evidenced by the highest rates of vertical instability and proximal translocation of the odontoid in later stages of infection.

Proposed Pathogenesis of CVJ Tuberculosis

Based upon these data, we conjecture the following pathogenesis for CVJ tuberculosis. Early-stage disease begins with hematogenous seeding of the synovium of any of the 5 synovial joints of the CVJ (2 occipitoatlantal, 2 atlantoaxial, and 1 atlanto-dental). Most of the literature states that the infection starts in the retropharyngeal space and then secondarily involves the bone similar to what happens in Grisel syndrome, where atlantoaxial subluxation develops after a bout of

pharyngitis.^{10,18} However, the imaging evidence here shows that the cold abscess never invades the retropharyngeal space. In the early stages of the infection, the abscess exclusively localizes to the prevertebral space around the synovial CVJ joints. In addition, the pattern of anatomic localization of osteomyelitic lesions supports origination in the synovium, as anatomic structures with an articulating synovial surface (lateral masses of C1, occipital condyles, C2 superior facets, and odontoid) are not only involved early in the disease but also show the most severe destruction. Areas of the CVJ without an articulating synovial surface (clivus, C2 body, posterior elements) seem to become involved secondarily through the contiguous spread of infection from articulating sites. Such a pathogenesis is consistent with the well-known predilection of *Mycobacterium tuberculosis* for synovial tissue and the documentation of a similar pattern of destruction in infections of the large joints of the appendicular skeleton.¹⁹ Based upon this proposed pathogenesis, we propose 3 stages (Table 3).

Stage I (Figure 2A-H) is characterized by infective synovitis of any of the CVJ joints with minimal or no bony destructions. Ligaments are intact and hence there is no instability. Clinical symptoms typically include neck pain and stiffness (especially to rotations), and rarely torticollis. The torticollis is either due to muscle spasms or rotatory atlantoaxial subluxation without AP instability. In the absence of instability, neurological deficit is extremely rare and a review of the literature failed to demonstrate a case of CVJ TB causing neurological deficits without some degree of instability. We conjecture that this may be due to the relatively capacious central canal at the CVJ, which affords significant abscess growth prior to cord compression. Consequently, epidural abscess in the absence of instability at the CVJ rarely causes mechanical cord compression.

Stage II (Figure 3A-F) is a distinct stage in the pathogenesis of the disease wherein the bone destruction is minimal or absent but the ligamentous stabilizers are sufficiently damaged to cause AP instability. Proximal translocation of odontoid is not seen in this stage as the lateral weight bearing columns and C1 ring are intact. Autopsy findings have shown the infection to progressively infiltrate and disrupt the transverse ligament and capsular structures.²⁰ This finding can be correlated to tuberculous involvement of other synovial joints in the extremities where it damages the capsular and ligamentous constraints before grossly destroying bone.¹⁹

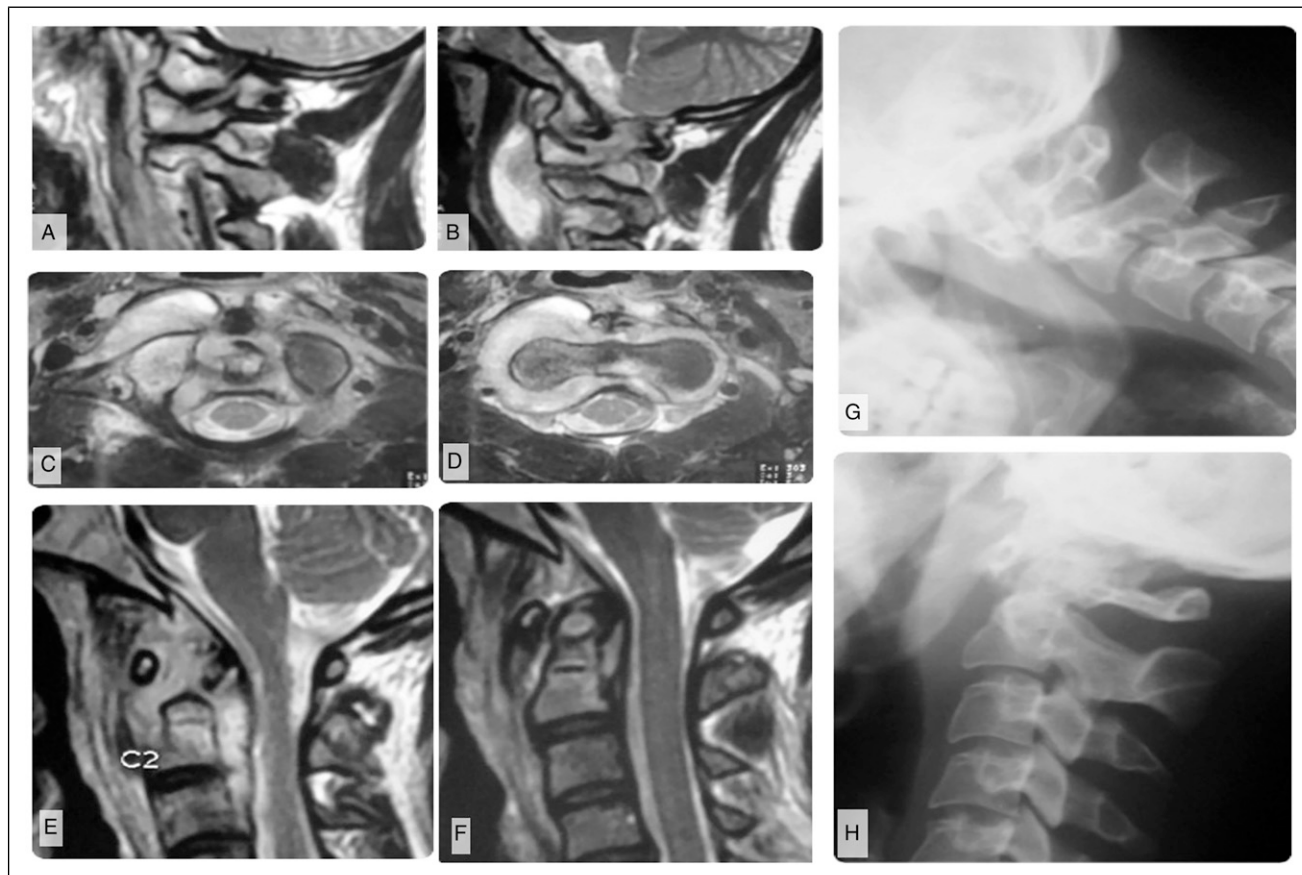


Figure 2. Imaging of a patient with modified Lifeso Stage I disease. (A) Parasagittal MRI shows abscess formation around the lateral atlantoaxial joints and (B) elevation of the prevertebral musculature. (C–D) Demonstrates that the abscess does not violate the prevertebral fascia, but may track into the epidural space through the neural foramina. (E) Parasagittal T2-weighted MRI shows that the abscess preferentially involves sites with an articular surface but (F) sagittal images show no ligamentous incompetence or bony destruction. This is similarly reflected on (G) flexion and (H) extension plain films.

Rotatory subluxation, if present, is associated with AP instability and this can present as torticollis. The cause of neurological deficit in this stage is primarily due to AP instability with or without epidural abscess.

Stage III (Figure 4A-L) represents the most advanced stage of disease and is characterized by severe destruction of bony anatomy. The destruction compromises the integrity of 2 main articulating structures: 1) the pivot joint between C1 and C2 (atlanto-dental joint) and 2) the 2 lateral weight bearing columns. Destruction of the bone contributing to the atlanto-dental joint viz. the odontoid process and the anterior C1 arch, results in AP instability (subtype Stage IIIA). Two types of odontoid destructive lesions were noted: 1) pathological fracture, and 2) complete destruction of the odontoid peg.² Vertical instability or proximal translocation of the dens is noted when the lateral supporting columns of the CVJ are damaged (Stage IIIB). The lateral mass bears the brunt of destruction being in the middle of 2 large synovial joints. Moreover, since the transverse ligament is inserted on the lateral mass of atlas, damage to these structures also

compromises the atlanto-dental joint stability and results in worsening of cord compression by a combination of vertical and AP instability. Hypoglossal nerve palsy can occur due to injury to the nerve as it traverses through a foramen at the base of the occipital condyle. Patients in this stage may present with torticollis due to unequal collapse of the lateral weight bearing columns (Figure 4A-L).

Previous Grading Systems

Several other grading schemas have been developed (Table 4). Lifeso¹⁰ presented one of the early descriptions of CVJ tuberculosis, which he divided disease into 3 stages based upon the degree of radiographic anterior atlantoaxial dislocation. This system is a popular classification schema used in many prior descriptions of CVJ TB.^{8,21,22} In Stage I disease, the ligaments are intact, there is minimal bone destruction, and no evidence of anterior displacement of C1 over C2. In Stage II, there is ligamentous disruption with anterior displacement of C1 on C2, but with minimal or no bony destruction. In stage III

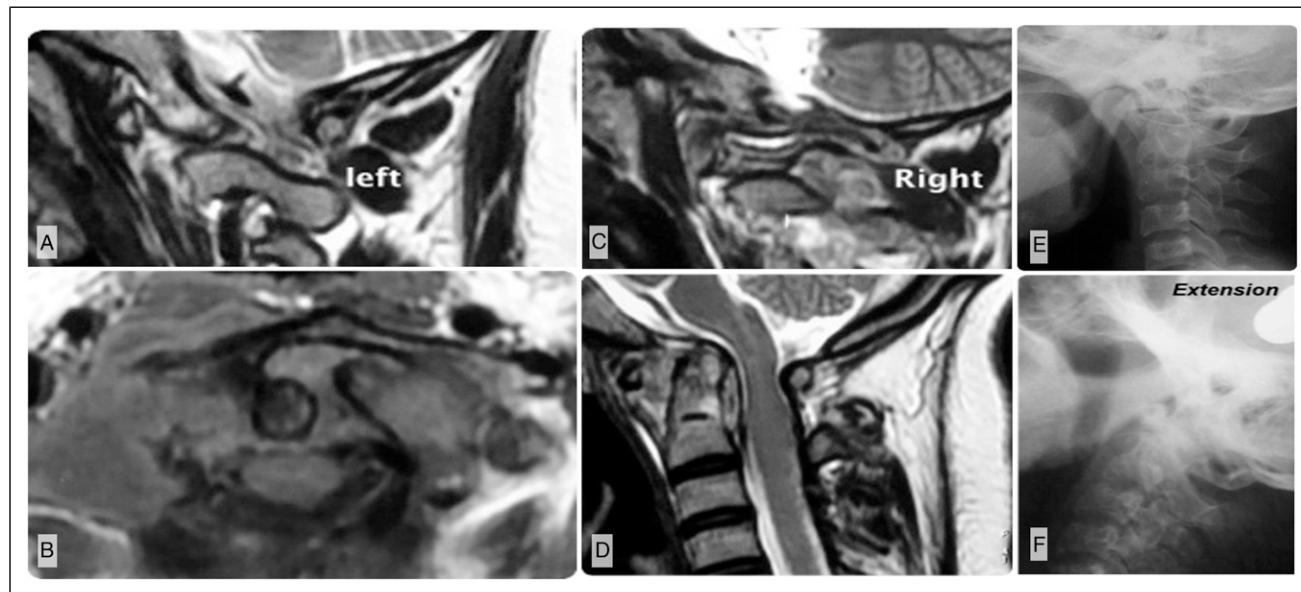


Figure 3. Imaging of a patient with modified Lifeso stage II disease. A–B) Parasagittal T2-weighted MRI showing the left and right lateral bony pillars are intact. C) Axial MRI illustrates disruption of the transverse atlantal ligament. D) Sagittal T2-weighted MRI shows the odontoid remains intact though there has been enlargement of the atlanto-dental interval (ADI) consistent with antero-posterior instability. E–F) Flexion and extension views similarly illustrate an enlarged ADI and antero-posterior instability.

disease, there is marked bone destruction with complete obliteration of the anterior C1 arch, and eventually complete destruction of the odontoid.¹⁰ Those with Stage I disease were treated conservatively in Lifeso's report, while those with Stage II/III disease were treated operatively. Neither rotatory nor vertical subluxation were considered in the schema.

While Lifeso's classification provides a fair understanding of the pathogenesis of the disease, the author made some contradictory observations with respect to proximal translocation of the dens (basilar impression). Of the 12 patients, 1 with 14 mm of proximal translocation of the dens above the McRae line was classified as Stage I, and was the only Stage I patient treated aggressively using a Halo vest.¹⁰ Similarly, another patient with 4 mm of proximal odontoid translocation was classified as Stage II.¹⁰ Such proximal translocation of the dens above McRae's line is only possible if there is significant destruction of the lateral pillars, which are the only load-bearing columns of the CVJ. As Lifeso Stage I and II lesions are defined by the absence of bone destruction, this case is similarly misclassified. Basilar impression (proximal translocation of the odontoid) due to CVJ TB is a severe deformity requiring aggressive management and should accordingly not be grouped with Stage I or II disease. The fact that CVJ TB can result in a serious deformity such as vertical translocation of the odontoid into the foramen magnum has been left out by most radiological classifications published to date.^{3,6,7,23}

Khandelwal and colleagues^{6,23} proposed a three-tiered system based strictly on radiographic criteria. All stages presented with a retropharyngeal abscess; however, stage II was distinguished from stage I by the presence of mild bony

erosion, and stage III was distinguished from stage II by gross bony destruction or angulation. Unlike Lifeso, anterior atlantoaxial dislocation (AAD) was not incorporated into lesion grading as all patients were noted to have some degree of anterior AAD. Furthermore, the authors reported that among their contemporary series of 16 patients, all were treated conservatively, suggesting that the grading paradigm may be ineffective for identifying operative candidates.

A decade later, Behari et al.³ described their experience of 25 patients with CVJ tuberculosis. Patients were graded based upon the severity of myelopathy at presentation and the presence of radiographic AAD. It did not consider the severity of bone destruction or the presence of deformity though. Patients with no or mild neurological deficit without AAD or fixed AAD were treated conservatively and those with reducible AAD were operated. All patients presenting with severe deficits were treated surgically. Similarly, Teegala et al.⁷ published the All India Institute of Medical Sciences (AIIMS) Grading system. Like the score of Behari et al.,³ the AIIMS system is a clinico-radiological grading system. Unlike Behari et al.³ though, the authors tried to radiologically categorize the severity of bone destruction with severe bone destruction defined as involvement of more than 1 Denis vertebral column.²⁴ However, the three-column concept of Denis has poor applicability at the CVJ, where there are only 2 lateral weight bearing columns.

Most recently, Goel^{25,26} described a three-stage system designed to model natural progression. Stage I disease is characterized by infection of the cancellous bone of 1 C1 facet, which may be accompanied by periarticular abscess formation.

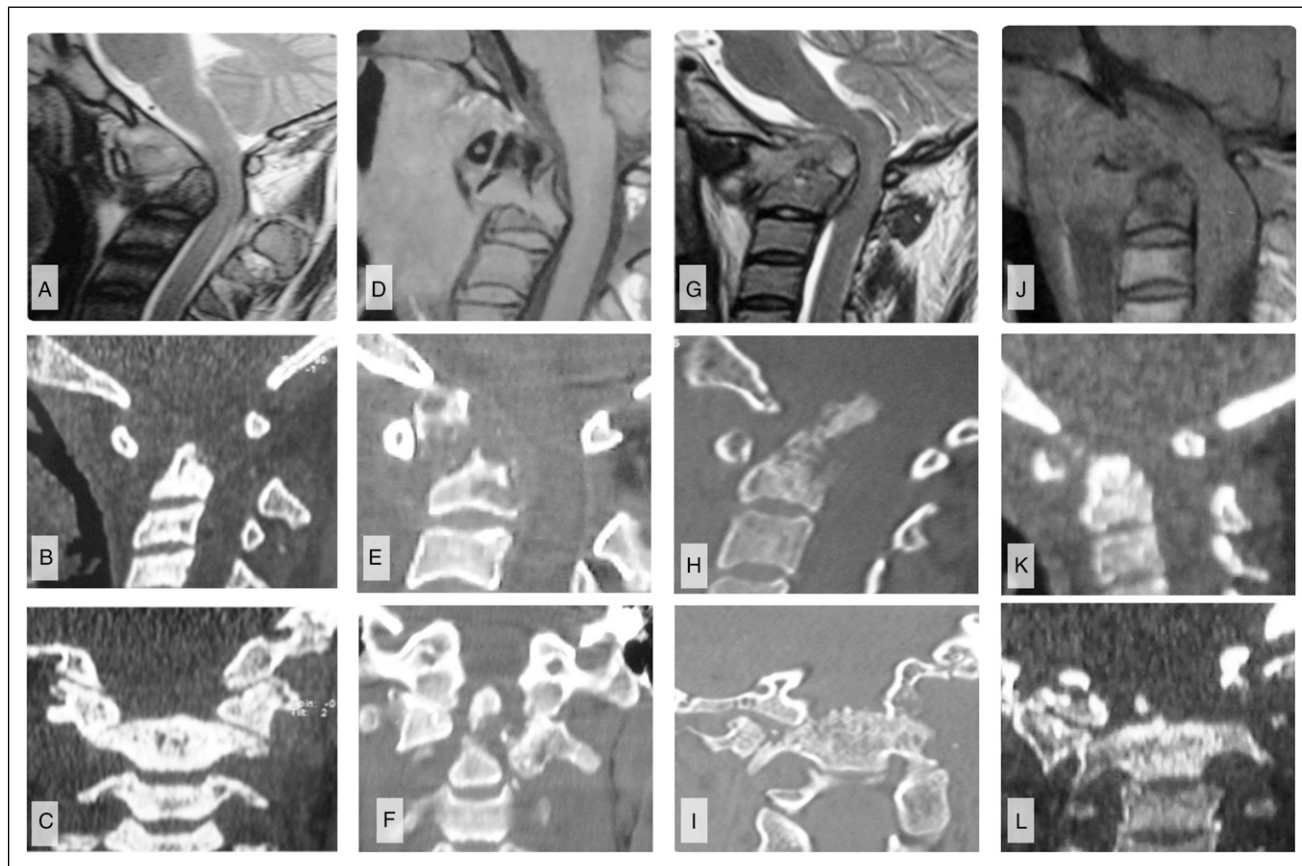


Figure 4. Imaging of 4 cases of modified Lifeso stage III disease. A–C) Case 1. A) Mid-sagittal T2-weighted MRI shows odontoid process destruction with anterior angulation of the occipitoatlantal junction and cervical cord impression. B) Sagittal CT imaging confirms the bony destruction with widening of the ADI, but C) coronal views show that the lateral bony pillars remain intact. D–F) Case 2. D) T1-weighted MRI and E) sagittal CT show odontoid process destruction with angulation of the craniovertebral junction, but less severe compression of the cervical cord. F) Coronal CT again illustrates the lateral bony pillars to be intact. G–I) Case 3. G) Sagittal T2-weighted MRI and H) sagittal CT images show odontoid destruction with vertical instability resulting in translocation of the odontoid through the foramen magnum, causing cervicomedullary cord compression with resultant T2-weighted signal change. I) Coronal CT illustrates that this vertical instability is accompanied by destruction of the lateral bony pillars. J–L) Case 4. J–K) Consistent with other stage III disease, sagittal T1-weighted MRI and CT show odontoid destruction; there is also craniovertebral settling consistent with vertical instability. L) Coronal CT demonstrates that there is destruction of the lateral bony pillars, explaining the vertical instability.

In stage II, there is progressive destruction of the unilateral atlantoaxial joint, often accompanied by ligamentous incompetence and anterior atlantoaxial dislocation. Finally, in stage III there is bilateral atlantoaxial joint destruction with atlantoaxial instability and generally both mechanical pain and neurological deficits. In our imaging study, we have identified several patients with bilateral joint involvement who are in Stage I and Stage II. Although this staging possesses many similarities to the present radiographic staging system, we argue that there is at least one important distinction. That is the present system distinguishes between vertical dislocation/subluxation of the dens (craniocervical deformity) and isolated anterior-posterior subluxation (instability). With medical management of the underlying infection and cervical stabilization (i.e., with halo vest or bed rest and traction), isolated anterior-posterior subluxation may heal and allow the patient to avoid operative intervention. However, vertical subluxation appears to

only occur secondary to destruction of the lateral bony pillars; this deformity will not resolve even with clearance of the infection and therefore represents an operative indication. This is acknowledged in Goel's publication;²⁶ however, the authors' system does not distinguish anterior-posterior and vertical subluxation, which the present system incorporates, given its potential to alter patient management.

Limitations

There are several limitations to this study. First, while this series is one of the largest single-center series published to date on CVJ tuberculosis, it is a relatively small sample and the results may therefore not be generalizable. Multidrug-resistant TB is on the rise and can present with unexpected patterns. Although our modification of the Lifeso grading describes a logical progression of

Table 4. Classification schemas for craniovertebral junction tuberculosis.

Schema	N	Stage I†	Stage II†	Stage III†	Stage IV†	Notes
Lifeso 1987 ¹⁰	12	Ligaments intact No anterior AAD ±rotatory ± vertical AAD	Ligamentous disruption Anterior ± rotatory ± vertical AAD	Ligamentous disruption Anterior ± rotatory ± vertical AAD	N/A	
Khandelwal et al. 1991 ⁶	51	No bone destruction RP abscess AAD	Minimal bone destruction RP abscess ±AAD	Marked bone destruction including anterior C1 arch RP abscess ± AAD	N/A	
Behari et al. 2003 ³	25	No bone erosion Neck pain No pyramidal symptoms	Mild bone destruction Neck pain Minor pyramidal symptoms	Gross bone destruction or angulation Neck pain Pyramidal symptoms	Neck pain Pyramidal symptoms	No radiographic criteria
AIIMS system 2008 ⁷	71	Functionally independent Score 3–4 Neck movement restriction No I Yes 2	Functionally independent Score 5–6 Motor score No weakness I MRC ≥ 4 2 MRC ≤ 3 3	Partial functional dependence with ADLs Score 7–8 Radiographic score C2 RP abscess without instability or bone erosion RP abscess with bony destruction and thecal sac compression without cord compression or signal change Severe bone destruction with cord compression or signal change	Complete functional dependence N/A	Composite score is sum Of motor, radiographic, and neck Movement scores
Goel 2016 ²⁵	N/A	Unilateral of cancellous bone of C1 facet No deformity ± Abscess Neck pain No neuro deficits	Unilateral atlantoaxial joint destruction Ligamentous disruption ± anterior AAD ± Abscess Neck pain + restriction of movement + torticollis ± neuro deficits Synovitis Ligamentous incompetence Bone lesions without erosion	Bilateral atlantoaxial joint destruction Atlantoaxial instability ± Abscess ± mechanical neck pain Usually neuro deficit Synovitis Ligamentous incompetence Bone lesions with erosion	N/A	
Present schema	52	Synovitis No ligamentous incompetence No bony erosion No AAD No myelopathy Neck pain Abscess often present	Synovitis Ligamentous incompetence Bone lesions without erosion Anterior ± rotatory AAD Myelopathy common Neck pain (±mechanical) Abscess generally present	Synovitis Ligamentous incompetence Bone lesions with erosion Vertical AAD ± anterior ± rotatory AAD Myelopathy common Neck pain (±mechanical) Abscess generally present	N/A	Stage 3A – Anterior AAD present Stage 3B – vertical AAD Present

Key: AAD—atlantoaxial dislocation; ADL—activities of daily living; AIIMS—All India Institute of Medical Sciences; MRC—motor research council; N/A—not applicable; RP—retropharyngeal.

Note: †The grades identified in the present table are not necessarily equivalent (e.g., a grade I lesion in the Khandelwal et al. 1992 system is not necessarily equivalent to a grade I lesion in the system we propose here). They are presented in this manner to help concisely illustrate the stages in each described system and the factors used to define the stages.

destruction, it may not be possible always to assign an individual patient to a particular stage as the radiological spectrum is a part of a continuum.

Conclusion

Based upon the present results, we argue for a pathogenesis of CVJ tuberculosis in which it originates in the CVJ joint peri-articular synovium. It subsequently spreads to the ligaments, creating ligamentous incompetence, and finally invades the bone with destruction of the lateral pillars and odontoid. To reflect this, here we propose a modified Lifeso classification wherein stage I constitutes infective synovitis without instability. Stage II is characterized by TAL incompetence and dynamic instability without CVJ deformity. Lastly, stage III is characterized by bony destruction with associated instability, which may be accompanied by deformity secondary to proximal translocation of the odontoid. Further validation based upon multi-institutional collaborations is merited.

Author's Notes

A portion of the present results were previously presented at the 2018 Cervical Spine Research Society Asia Pacific Meeting in New Delhi, India, and at the Radiological Society of North America 98th Scientific Assembly and Annual Meeting in 2012 in Chicago, Illinois.

Declaration of Conflicting Interests

The author(s) declared no potential conflicts of interest with respect to the research, authorship, and/or publication of this article.

Funding

The author(s) received no financial support for the research, authorship, and/or publication of this article.

Ethical approval

IRB approval was obtained prior to initiation of the present study. The IRB deemed "Proposed study activities do not meet the definition of human subject research, and therefore are deemed to be not human subjects research."

ORCID iDs

Kshitij Chaudhary  <https://orcid.org/0000-0002-4879-1636>
 Zach Pennington  <https://orcid.org/0000-0001-8012-860X>
 Daniel M. Sciubba  <https://orcid.org/0000-0001-7604-434X>
 Sanjeev Suratwala  <https://orcid.org/0000-0002-8701-0740>

Supplemental Material

Supplemental material for this article is available online.

References

1. Kracht J. Tuberculosis of the atlas and axis. *Beitr Klin Tuberk Spezif Tuberkuloseforsch.* 1950;104(4):307-310. <http://www.ncbi.nlm.nih.gov/pubmed/14791249>
2. Chaudhary K, Potdar P, Bapat M, Rathod A, Laheri V. Structural odontoid lesions in craniovertebral tuberculosis. A review of 15 cases. *Spine (Phila Pa 1976).* 2012;37(14):E836-E843. doi:10.1097/BRS.0b013e31824a4c8f.
3. Behari S, Nayak SR, Bhargava V, Banerji D, Chhabra DK, Jain VK. Craniocervical tuberculosis: protocol of surgical management. *Neurosurgery.* 2003;52(1):72-80. discussion 80-1. doi:10.1227/0006123-200301000-00009.
4. Tuli SM. Tuberculosis of the craniovertebral region. *Clin Orthop Relat Res.* 1974;104:209-212. doi:10.1097/00003086-197410000-00023.
5. Molliqaj G, Dammann P, Schaller K, Sure U, Tessitore E. Management of craniovertebral junction tuberculosis presenting with atlantoaxial dislocation. *Acta Neurochirurgica. Supplement,* 2019;125;2019:337-344. doi:10.1007/978-3-319-62515-7_49. Springer
6. Gupta SK, Mohindra S, Sharma BS, et al. Tuberculosis of the craniovertebral junction: is surgery necessary? *Neurosurgery.* 2006;58(6):1144-1150. doi:10.1227/01.NEU.0000215950.85745.33.
7. Teegala R, Kumar P, Kale SS, Sharma BS. Craniovertebral junction tuberculosis: a new comprehensive therapeutic strategy. *Neurosurgery.* 2008;63(5):946-955. doi:10.1227/01.NEU.0000327696.77814.1E.
8. Arora S, Sabat D, Maini L, et al. The results of nonoperative treatment of craniovertebral junction tuberculosis: a review of twenty-six cases. *J Bone Jt Surgery-American.* 2011;93(6):540-547. doi:10.2106/JBJS.J.00634.
9. Zhang Y, Wu Y, Fu S, et al. Treatment of tuberculosis in craniovertebral junction. *Zhongguo Xiu Fu Chong Jian Wai Ke Za Zhi.* 2020;34(12):1507-1514. doi:10.7507/1002-1892.202005087.
10. Lifeso R. Atlanto-axial tuberculosis in adults. *J Bone Joint Surg Br.* 1987;69-B(2):183-187. doi:10.1302/0301-620X.69B2.3818746.
11. Ahuja K, Gupta T, Ifthekar S, Mittal S, Yadav G, Kandwal P. Variability in management practices and surgical decision making in spinal tuberculosis: an expert survey-based study. *Asian Spine J.* 2021. Published online;1. doi:10.31616/asj.2020.0557.
12. Frankel HL, Hancock DO, Hyslop G, et al. The value of postural reduction in the initial management of closed injuries of the spine with paraplegia and tetraplegia. *Spinal Cord.* 1969;7(3):179-192. doi:10.1038/sc.1969.30.
13. Menezes AH, Traynelis VC. Anatomy and biomechanics of normal craniovertebral junction (a) and biomechanics of stabilization (b). *Child's Nerv Syst.* 2008;24(10):1091-1100. doi:10.1007/s00381-008-0606-8.
14. McRae DL, Barnum AS. Occipitalization of the atlas. *Am J Roentgenol Radium Ther Nucl Med.* 1953;70(1):23-46. <https://www.ncbi.nlm.nih.gov/pubmed/13058024>
15. Pai M, Behr MA, Dowdy D, et al. *Tuberculosis.* *Nat Rev Dis Prim.* 2016;2(1):16076. doi:10.1038/nrdp.2016.76.
16. De la Garza Ramos R, Goodwin CR, Abu-Bonsrah N, et al. The epidemiology of spinal tuberculosis in the United States: an

- analysis of 2002–2011 data. *J Neurosurg Spine*. 2017;26(4):507-512. doi:10.3171/2016.9.SPINE16174.
17. Rajasekaran S, Soundararajan DCR, Shetty AP, Kanna RM. Spinal tuberculosis: current concepts. *Global Spine J*. 2018; 8(4_suppl 1):96S-108S. doi:10.1177/2192568218769053.
 18. Jain AK, Kumar S, Tuli SM. Tuberculosis of spine (C1 to D4). *Spinal Cord*. 1999;37(5):362-369. doi:10.1038/sj.sc.3100833.
 19. Tuli SM. *Tuberculosis of the Skeletal System (Bones, Joints, Spine and Bursal Sheaths)*. 4th ed. Jaypee Brothers Medical Publishers Ltd; 2010.
 20. Pandya SK. Tuberculous atlanto-axial dislocation (with remarks on the mechanism of dislocation). *Neurol India*. 1971;19(3):116-121. <http://www.ncbi.nlm.nih.gov/pubmed/5157880>
 21. Shukla D, Mongia S, Devi BI, Chandramouli BA, Das BS. Management of craniovertebral junction tuberculosis. *Surg Neurol*. 2005;63(2):101-106. doi:10.1016/j.surneu.2004.03.019.
 22. Chadha M, Agarwal A, Singh AP. Craniovertebral tuberculosis: a retrospective review of 13 cases managed conservatively. *Spine (Phila Pa 1976)*. 2007;32(15):1629-1634. doi:10.1097/BRS.0b013e318074d41e.
 23. Khandelwal N, Khosla VK, Malik N, Radotra BD, Kak VK, Suri S. Tuberculous atlanto-axial dislocation. In: Proceedings of the XIV Symposium Neuroradiologicum, London, 17–23 June 1991. Springer Berlin Heidelberg:106-108. doi:10.1007/978-3-642-49329-4_35.
 24. Denis F. Spinal instability as defined by the three-column spine concept in acute spinal trauma. *Clin Orthop Relat Res*. 1984; 189:65-76. <https://www.ncbi.nlm.nih.gov/pubmed/6478705>
 25. Goel A. Tuberculosis of craniovertebral junction: role of facets in pathogenesis and treatment. *J Craniovertebral Junction Spine*. 2016;7(3):129. doi:10.4103/0974-8237.188418.
 26. Goel A, Goel NK, Shah A. Pathogenesis of tuberculosis of the craniovertebral junction: its implication in surgical management. In: Goel A, Cacciola F, eds. *The Craniovertebral Junction: Diagnosis, Pathology, Surgical Techniques*. 1st ed. Georg Thieme Verlag; 2011:415-422. doi:10.1055/b-0034-81414.